Chaotic motion of diffuse domain walls in magnetic garnets

Robert A. Kosiński
Institute of Physics, Warsaw University of Technology, Koszykowa 75, 00-662 Warsaw, Poland
(Received 19 April 1994)

The motion of diffuse domain walls in thin garnet films (i.e., walls with extreme width), which was observed experimentally when an in-plane magnetic field was applied, is analyzed numerically using a spatiotemporal diagram technique and analysis of the time evolution of pattern entropy. It is found that the motion of such walls is chaotic and experimental observations of diffuse domain walls may be treated as a direct observation of chaotic motion in a magnetic system.

I. INTRODUCTION

One of the most interesting spatially extended magnetic systems is domain walls in thin magnetic films. They were investigated extensively for years because of their interesting physical properties as well as because of applications in magnetic recording and computer memories. A large number of experimental and theoretical works was devoted to the dynamic properties of such walls (see, for example, Ref. 1 and references therein). In particular, it was found theoretically that, depending on the values of external field and material parameters, domain-wall motion may be chaotic.[2–4] On the other hand, experimental observations of domain wall dynamics analyzing it from the point of view of chaotic wall motion were made rather for the case of a periodic drive field.[5–7]

An interesting phenomenon was found by Zimmer, Morris, Vural, and Humphrey in the experimental observation of the motion of domain walls in a thin garnet film with a properly oriented in-plane magnetic field (H_y).[8] Such a wall became extremely wide in comparison with its static width and was called a "diffuse wall." It was suggested that this phenomenon results from the complex internal structure of the wall: horizontal Bloch lines of very large angular span appear in the wall and its surface is significantly deflected from the initial orientation of wall plane and direction of observation.[8–10] The internal structure of the diffuse walls was confirmed by numerical simulations of wall motion based on solution of the equations of motion.[11] The average width of the wall Δ as a function of time obtained in these computations agrees very well with the experimental observations of $\Delta(t)$.[11]

In the present paper it is shown, using numerical analysis of domain-wall dynamics, that the appearance of a diffuse domain wall is a result of chaotic motion. The spatiotemporal diagram technique and time evolution of pattern entropy $S(t)$ were applied for quantitative investigations of wall motion.[12,13]

II. NUMERICAL ANALYSIS

A twisted domain wall in uniaxial magnetic bubble garnet is considered (Fig. 1). The motion of such a wall is described by a pair of partial, nonlinear differential equations derived from the Landau-Lifshitz equation with a Gilbert damping term included.[14] After a number of simplifying assumptions (for details, see Ref. 1) the equations of wall motion have the form proposed by Slonczewski:[15]

$$\frac{\dot{q}}{\Delta_0}=2\pi M\gamma \sin 2\psi-\frac{2A\gamma}{M}\psi_{zz}+\frac{\gamma K}{M}\sin 2\psi + \frac{\gamma\pi}{2}H_{sy}\sin 2\psi+\alpha\dot{\psi}\ , \tag{1}$$

$$\dot{\psi}=\gamma H_z+\frac{2\gamma A}{M\Delta_0}q_{zz}-\frac{\alpha}{\Delta_0}\dot{q}\ . \tag{2}$$

Here, A is the exchange constant, γ is the gyromagnetic ratio, M is the saturation magnetization, α is the Gilbert damping constant, $\Delta_0=\sqrt{A/K}$ is the wall width parameter (K is the uniaxial perpendicular anisotropy constant), and H_z is the constant drive field applied to the film. In Eqs. (1) and (2), $q(z,t)$ describes the local position of the wall and the azimuthal angle $\psi(z,t)$ describes the direction of the local magnetic moment of the wall with respect to the $+0x$ axis (Fig. 1). A dot over a symbol denotes the time derivative and the subscript zz the second derivative with respect to the z coordinate. H_{sy} denotes the stray field due to the surfaces of the film and is calculated here according to the model proposed by Hagedorn.[16]

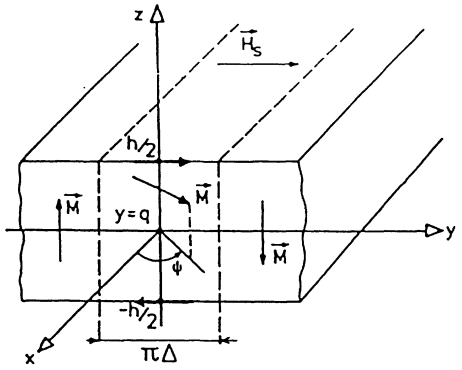

FIG. 1. Domain wall in thin film of thickness h. M is the magnetization, H_s is the stray field, Δ is the wall width, ψ is the azimuthal angle of magnetization, and q denotes the wall position.

The equations of motion (1) and (2) were solved by means of a full implicit numerical scheme with a grid of $N=52$ numerical points spaced uniformly along the film thickness h (details are described in Ref. 17). Force-free boundary conditions were applied.[1] The initial conditions were $q(z,0)=0$, $\psi(z,0)=\psi_s(z)$, where $\psi_s(z)$ is the static distribution for the twisted wall.

For preliminary control of the type of wall motion the character of the phase trajectory $\tilde{\psi}(\tilde{q})$ in a chosen phase subspace of the wall was observed. Here, the tilde denotes that the values of $\bar{q}$ and $\bar{\psi}$, averaged over the film thickness, were subtracted from the instantaneous values of q_{mid} and ψ_{mid} of the middle grid point of the wall, respectively. Such a phase trajectory $\tilde{\psi}(\tilde{\psi})$ is shown in Fig. 2 and its character will be discussed later.

For quantitative analysis of the wall motion a spatiotemporal diagram technique was used. It was initially developed for a rather simple dynamic system.[12,18] Next, it was also applied to complex systems described by partial differential equations of wall motion (see, for instance, Ref. 13). The construction of the spatiotemporal diagrams was based on the numerical solutions of Eqs. (1) and (2), where the variable $\psi_i(t)$— at each numerical point ($i=1,\ldots,N$)—was used. Its time evolution was digitized using the following rule: in each nth time step of the integration procedure ΔT ($\Delta T=0.1$ nsec) the value 0 or 1 was assigned to the ith grid point if $|\psi_i|<|\bar{\psi}|$ or $|\psi_i|\geq|\bar{\psi}|$, respectively. $\bar{\psi}$ denotes here the spatial average of $\psi(z)$ over the film thickness. Thus, each sequence of 0's and 1's obtained for a given grid point instead of the sequence of solutions $\psi_i(n\Delta T)$ ($n=100,200,300,\ldots$) yielded the necessary information to discern the type of wall motion. Spatiotemporal diagrams for the whole segment of the wall were constructed as sets of the sequences of white (for 0) and black (for 1) cells of size $[\Delta z=h/(N-1),\ \Delta t=100\Delta T]$ for all grid points (see Fig. 3). As we will see below, such spatiotemporal diagrams display clearly the type of wall motion (however, also other sequences of n like $n=250,500,750,\ldots$ may also be chosen).[13]

For the synthetic characterization of spatiotemporal diagrams, the pattern entropy S proposed by Kaneko[12] and Crutchfield and Kaneko[18] and calculated for each spatiotemporal diagram was used.[13] It is defined as

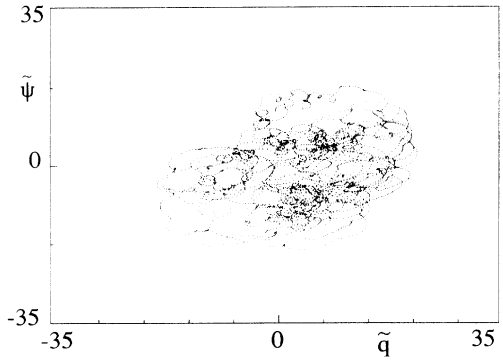

FIG. 2. Phase trajectory $\tilde{\psi}(\tilde{q})$ for in-plane perpendicular field $H_y=200$ Oe. $H_z=135$ Oe, $H_x=0$ Oe, and $15<t<600$ nsec.

FIG. 3. Spatiotemporal diagram for $H_z=135$ Oe, $H_y=200$ Oe, $H_x=0$. The vertical direction corresponds to the $+0z$ axis, and the time axis is parallel to the horizontal direction. One white or black cell has vertical dimension $\Delta z=h/(N-1)=h/51$ and horizontal dimension $\Delta t=100\Delta T=10$ nsec. The time interval of wall motion $200<t<700$ nsec is shown in this figure.

$$S=\sum_j \frac{p_j}{K}\ln\frac{p_j}{K}\ , \tag{3}$$

where p_j is the probability of the occurrence in the pattern of a sequence of 1's (called below "pattern domains") of length j, calculated in the direction of film thickness ($0z$ axis). K is the total number of pattern domains in the whole pattern. During wall motion, the entropy is calculated for a sequence of patterns, each constructed according to the above recipe, for a chosen time window $t_w=100$ nsec.

In our computations, the values of external fields as well as the material parameters were the same as during experimental observations of wall motion performed by Vural and Humphrey:[9] exchange constant $A=1.547\times10^{-7}$ erg/cm, saturation magnetization $4\pi M=185$ G, gyromagnetic ratio $\gamma=1.1\times10^{7}$ sec^{-1} Oe^{-1}, Bloch wall width parameter $\Delta_0=2.611\times10^{-6}$ cm, Gilbert damping constant $\alpha=0.026$, and film thickness $h=6.8\times10^{-4}$ cm.

III. RESULTS FOR H_y FIELDS

As results from experimental and theoretical investigations show (see, for example, Ref. 1 and references therein), the relation between the wall velocity v and the drive field H_z in thin garnet films may be divided into two main regions. In the first region, when the drive field is smaller than a certain critical value $H_z=H_{z(\text{crit})}$, the relation $v(H_z)$ is linear and depends on the value of the external in-plane field.[19] In this region all magnetic moments of the wall deflect uniformly in the direction of the wall velocity v. In the second region, for H_z greater than $H_{z(\text{crit})}$, the wall velocity is a nonlinear function of H_z and often suddenly decreases.[1,17,19] This is caused by the appearance of complex internal structures in the wall, based

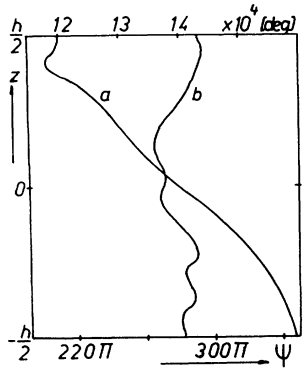

FIG. 4. Distribution of the azimuthal angle of magnetization $\psi(z)$ for $H_z=135$ Oe and $t=200$ nsec. Curve a, $H_y=200$ Oe, $H_x=0$; a horizontal Bloch line with very large angular span $\approx 150\pi$ is visible. Curve b, $H_x=200$ Oe, $H_y=0$; some horizontal Bloch lines with rather small angular span are present (Ref. 11).

on strong local precessions of magnetic moments and called horizontal Bloch lines. These structures have a dynamic character: their number, angular span, and position in the wall change during wall motion and depend on the values of external fields.[1,17,20]

Experimental observations of diffused walls were performed for $H_z=135$ Oe $>H_{z(\mathrm{crit})}$, i.e., deep in the nonlinear region of motion.[9] For the sample under consideration we found that $H_{z(\mathrm{crit})}(H_y=H_x=0)=0.345$ Oe and $H_{z(\mathrm{crit})}(H_y=200\ \mathrm{Oe})=1.8$ Oe. Moreover, the in-plane field applied to the moving wall used in the experiment ($H_y=200$ Oe or $H_x=200$ Oe) is relatively strong. It is sufficient for a strong desymmetrization of the $\psi(z)$ distribution and for a strong effect on the character of horizontal Bloch lines appearing in the wall.[11,17,20]

The phase trajectory for the case $H_z=135$ Oe and perpendicular in-plane field $H_y=200$ Oe is shown in Fig. 2 for the time interval $15<t<600$ nsec (15 nsec is the rise time of the drive field pulse.[9]) This time interval contains a transient motion which last some tenths of nanoseconds and is somewhat shorter than the interval observed in experiment $0<t<400$ nsec.[9] It can be seen that this trajectory is open, which is typical for chaotic motion. Also, spatiotemporal diagrams constructed for these values of external fields (see Fig. 3) have a nonregular character which reveals the chaotic type of wall motion. According to the coding of white and black cells described above, white stripes located in the upper and lower parts of the diagram (corresponding to upper and lower parts of the film) mean that the $\psi(z)$ values in these parts differ significantly from the average value $\bar{\psi}$. A horizontal Bloch line of very large angular span, exceeding 100π, is present in the wall (see curve a in Fig. 4). It is responsible for a very significant bending of the wall surface toward the direction of the H_y field and explains the increase of wall width Δ observed along the $0z$ axis. The wall width calculated from the solutions $q(z,t)$ and averaged in time (circles in Fig. 5) shows a very good agreement with the experiment (bars in Fig. 5).

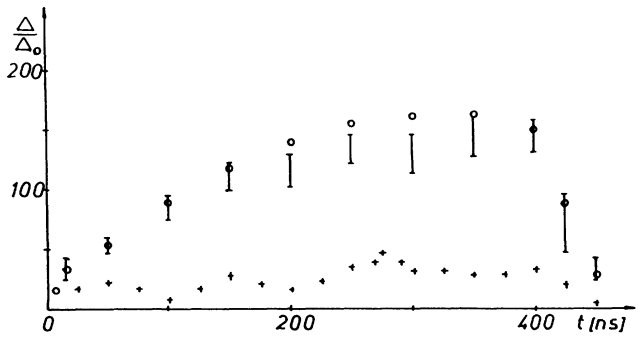

FIG. 5. Averaged wall width Δ (Δ_0 is the initial wall width parameter) as a function of time for perpendicular field $H_y=200$ Oe (circles) and parallel field $H_x=200$ Oe (crosses) obtained numerically in Ref. 11. Experimental results obtained in Ref. 9 are shown by vertical bars. The drive field is $H_z=135$ Oe.

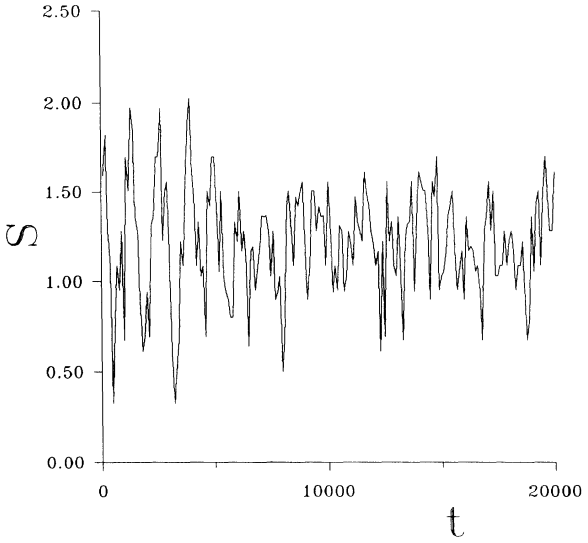

FIG. 6. Time evolution of the pattern entropy $S(t)$ for perpendicular in-plane field $H_y=200$ Oe (other values of external fields the same as in Fig. 2). Time window $t_w=100$ nsec was used.

The pattern entropy $S(t)$ calculated for the above values of the external fields is shown in Fig. 6. Sharp and

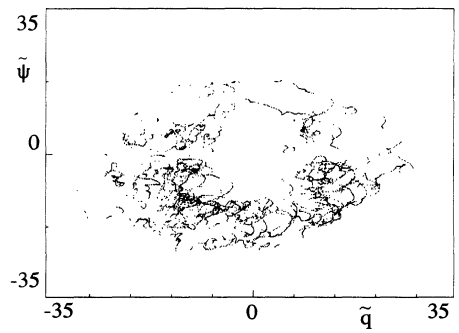

FIG. 7. Phase trajectory $\tilde{\psi}(\tilde{q})$ for in-plane field parallel to the wall $H_x=200$ Oe. Other field values were $H_y=0$, $H_z=135$ Oe, and $15<t<600$ nsec.

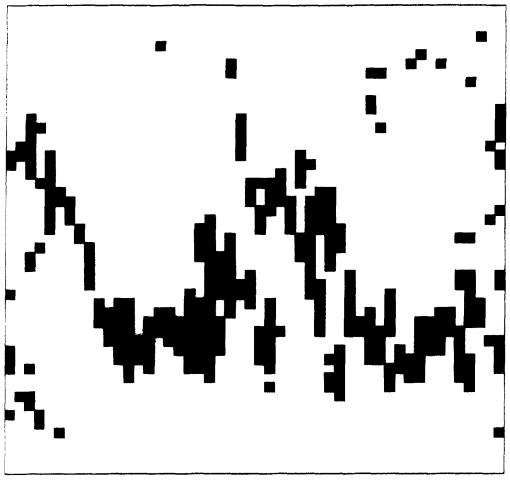

FIG. 8. Spatiotemporal diagram for in-plane field parallel to the wall (the values of all fields were the same as in Fig. 7). Orientation of the pattern as in Fig. 3.

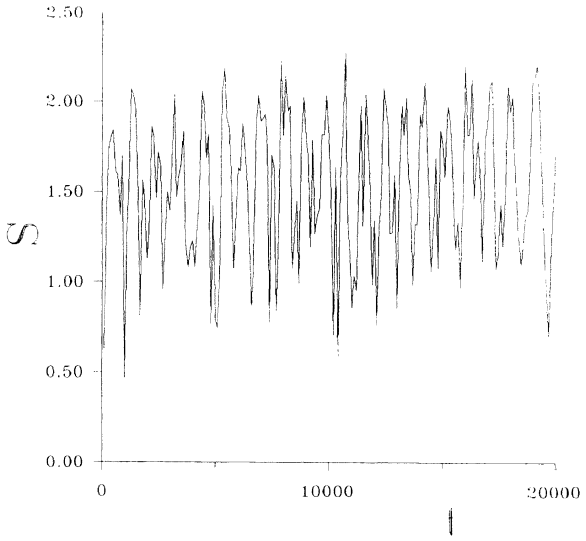

FIG. 9. Time evolution of the pattern entropy $S(t)$ for parallel in-plane field $H_x = 200$ Oe, calculated with the time window $t_w = 100$ nsec. (Other values of external fields are the same as in Fig. 7).

irregular oscillations of entropy prove the chaotic character of the motion of the wall.

IV. RESULTS FOR H_x FIELD

When an in-plane field parallel to the moving wall is applied the increase of average wall width observed in experiment[9] is much smaller than in the case of the H_y field (see crosses in Fig. 5). It was observed that numerical solutions $\psi(z,t)$ oscillate along the film thickness, which means that a number of horizontal Bloch lines, but with much smaller angular span than in the case of the use of H_y, are present in the moving wall (see curve b in Fig. 4). The average wall width Δ calculated from $q(z,t)$ solutions changes only slightly in comparison with its static value Δ_0. The phase trajectory $\bar{q}(\bar{\psi})$, calculated for $H_z = 135$ Oe and $H_x = 200$ Oe (the same as in experiment[9]), has an open character (Fig. 7). The spatiotemporal diagrams have much more complex character than in the case of H_y fields (Fig. 8). This is due to the large number of horizontal Bloch lines, which correspond to the number of transitions of $\psi(z)$ through its average value $\bar{\psi}$ (cf. curve b in Fig. 4). The time evolution of the pattern entropy $S(t)$ for the present case confirms the chaotic nature of the motion of the wall (Fig. 9). As results from the comparison of spatiotemporal diagrams for both H_y and H_x fields (Figs. 3 and 8), oscillations of the pattern entropy for H_x field are significantly larger than in the case of H_y fields.

V. CONCLUSIONS

It was found that the diffuse domain wall observed experimentally when an in-plane field perpendicular to the wall is applied to a garnet film[8-10] is a manifestation of the chaotic motion of the wall. Thus, the appearance of diffuse walls may be treated as a direct observation of chaotic motion a spatially extended magnetic system.

ACKNOWLEDGMENTS

The author wishes to thank Dr. J. Zebrowski for the critical reading of the manuscript and discussions. This work was supported by the KBN Grant No. 2-0250-91-1.

[1] A. P. Malozemoff and J. C. Slonczewski, *Magnetic Domain Walls in Bubble Materials* (American Press, New York, 1979).
[2] R. A. Kosinski, J. Appl. Phys. **73**, 320 (1993).
[3] J. Zebrowski, Phys. Scr. **38**, 632 (1988).
[4] J. J. Zebrowski and A. Sukiennicki, J. Appl. Phys. **56**, 249 (1984).
[5] L. M. Dedukh, V. Nikitenko, and V. T. Synogach, Zh. Eksp. Teor. Fiz. **94**, 312 (1988) [Sov. Phys. JETP **67**, 1912 (1988)].
[6] L. M. Dedukh, V. I. Nikitenko, and V. T. Synogach, Acta Phys. Polon. A **76**, 295 (1989).
[7] V. S. Gornakov, V. I. Nikitienko, I. A. Prudnikow, and V. T. Synogach, Phys. Rev. B **46**, 10 829 (1992).
[8] G. J. Zimmer, T. M. Morris, K. Vural, and F. B. Humphrey, Appl. Phys. Lett. **25**, 750 (1974).
[9] K. Vural and F. B. Humphrey, J. Appl. Phys. **51**, 549 (1980).
[10] T. Suzuki, L. Gal, and S. Maekawa, Jpn. J. Appl. Phys. **19**, 627 (1980).
[11] R. A. Kosinski, J. Phys. (Paris) Colloq. **49**, C8-1941 (1988).
[12] K. Kaneko, in *Formation Dynamics and Statistic of Patterns*, edited by K. Kawasaki *et al.* (World Scientific, Singapore, 1989).
[13] R. A. Kosinski, Phys. Lett. A **169**, 263 (1992).
[14] L. Landau and E. Lifshitz, Phys. Z. Soviet Union **8**, 153 (1935); T. L. Gilbert, Phys. Rev. **100**, 1243 (1955).

[15]J. C. Slonczewski, Int. J. Magn. **2**, 85 (1972).
[16]F. B. Hagedorn, J. Appl. Phys. **45**, 3129 (1974).
[17]R. A. Kosinski and J. Engemann, J. Magn. Magn. Mater. **50**, 229 (1985).
[18]J. P. Crutchfield and K. Kaneko, in *Directions in Chaos,* edited by H. Bai-Lin (World Scientific, Singapore, 1986).
[19]F. H. de Leeuv, R. van den Doel, and U. Enz, Rep. Prog. Phys. **43**, 690 (1980).
[20]R. A. Kosinski, IEEE Trans. Magn. **Mag-23**, 3373 (1987).